# Carbonylmetallates as versatile 2-, 4- or 6-Electron Donor Metalloligands in Transition-Metal Complexes and Clusters: A Global Approach

Noura Naili, Samia Kahlal, Bachir Zouchoune, Jean-Yves Saillard, Pierre Braunstein

10.1002/chem.202203557

WILEY-VCH

RESEARCH ARTICLE

# Carbonylmetallates as versatile 2-, 4- or 6-Electron Donor Metalloligands in Transition-Metal Complexes and Clusters: A Global Approach

Noura Naili,[a,b] Samia Kahlal,[c] Bachir Zouchoune,[a,d] Jean-Yves Saillard,*[c] and Pierre Braunstein*[e]

[a] Dr. Noura Naili, Dr. Bachir Zouchoune
Unité de Recherche de Chimie de l'Environnement et Moléculaire Structurale, Université Constantine (Mentouri), 25000 Constantine (Algeria)
[b] Dr. Noura Naili
Département de Chimie, Faculté des Sciences, Université de Skikda, 21000 Skikda (Algeria)
[c] Dr. Samia Kahlal, Prof. Dr. Jean-Yves Saillard
Université de Rennes, CNRS, ISCR-UMR 6226, 35000 Rennes (France)
E-mail: jean-yves.saillard@univ-rennes1.fr
[d] Dr. Bachir Zouchoune
Laboratoire de Chimie appliquée et Technologie des Matériaux, Université Larbi Ben M'Hidi-Oum El Bouaghi, 04000 Oum El Bouaghi (Algeria)
[e] Prof. Dr. Pierre Braunstein
Institut de Chimie (UMR 7177 CNRS), Université de Strasbourg, 4 rue Blaise Pascal, 67081 Strasbourg (France)
E-mail: braunstein@unistra.fr

Supporting information for this article is given via a link at the end of the document.

**Abstract:** Carbonylmetallates $[m]^-$, such as $[MoCp(CO)_3]^-$, $[Mn(CO)_5]^-$, $[Co(CO)_4]^-$, have long been successfully used in the preparation of hundreds of metal carbonyl complexes and clusters, in particular of the heterometallic type. We focus here on situations where $[m]^-$ can be viewed as a terminal, doubly- or even triply-bridging metalloligand, developing metal-metal interactions with one, two or three metal centres M, respectively. With metals M from the groups 10-12, it is not straightforward or even impossible to rationalize the structure of the resulting clusters by applying the well-known Wade-Mingos rules. A very simple but global approach is presented to rationalize structures not obeying usual electron-counting rules by considering the anionic building blocks $[m]^-$ as metalloligands behaving formally as potential 2, 4 or 6 electron donors, similarly to what is typically encountered with e.g. halido ligands. Qualitative and theoretical arguments using DFT calculations highlight similarities between seemingly unrelated metal complexes and clusters and also entail a predicting power with high synthetic potential.

## Introduction

Since heterometallic complexes and clusters began to attract the worldwide interest of dozens of research groups, carbonylmetallates $[m]^-$ ([m] = e.g. $Mo(\eta\text{-}C_5H_5)(CO)_3$, $Mn(CO)_5$, $Fe(CO)_3NO$, $Co(CO)_4$) have been used as metal-centered nucleophiles towards metal halide complexes $[MX_nL_m]$ to form direct metal-metal bonds M–[m] by displacement of one or more M–X bonds.[1] The relative nucleophilicity of these and related anions and the stability of the resulting metal-metal bonds were assessed back in 1966 in a series of detailed electrochemical investigations by Dessy and coll.[2] After the molecular structure of the trinuclear complex $[Hg\{Co(CO)_4\}_2]$ revealed a Co−Hg−Co chain structure,[3] systematic studies were performed by W. Hieber and coll. who isolated related Co−Zn−Co and Co−Cd−Co chain complexes,[4] and the research field developed very rapidly, including the synthesis, characterization and investigations of the properties of supported or unsupported metal-metal bonded complexes and metal clusters.[1,5-9] This synthetic procedure was also applied in 1964 by Coffey, Lewis and Nyholm to the synthesis of the first heterometallic complexes containing a metal–metal bond between a group 11 metal (Cu, Ag, Au) and another transition metal, such as W, Mn, Fe, or Co.[10] This dinuclear chemistry was extended to trinuclear chain complexes $\{[m]–Au–[m]\}^-$ ([m] = $CrCp(CO)_3$, $MoCp(CO)_3$, $Mn(CO)_5$, $FeCp(CO)_2$, $Co(CO)_4$; Cp = $\eta\text{-}C_5H_5$) (Figure 1).[11-14] Similarly, the use of these metallates $[m]^-$ provided access to chain complexes with a group 10 metal in the centre, [m]−$PtL_2$−[m] (L = 2e donor; [m] = $MoCp(CO)_3$,[11,15] $WCp(CO)_3$,[16] $Mn(CO)_5$,[11,16-21] $Co(CO)_4$,[11,17,19] $Fe(CO)_3NO$),[16,22] and their palladium analogs, which constituted the first examples of Pd−transition metal bonds (Figure 1).[11,15,18-20]

10.1002/chem.202203557




All these metal-metal bonded heterometallic complexes were obtained by nucleophilic substitution of one (for dinuclear complexes) or two (trinuclear complexes) M-bound halide ligands by the carbonylmetallate *anion*. The metal carbonyl fragment behaves in the product as a terminally bound metalloligand, acting as an anionic 2e donor, similarly to the halide ligand it replaces (alternatively, the metalloligand can be considered as behaving as a 1e neutral donor ligand, equivalent to a neutral halogen ligand).

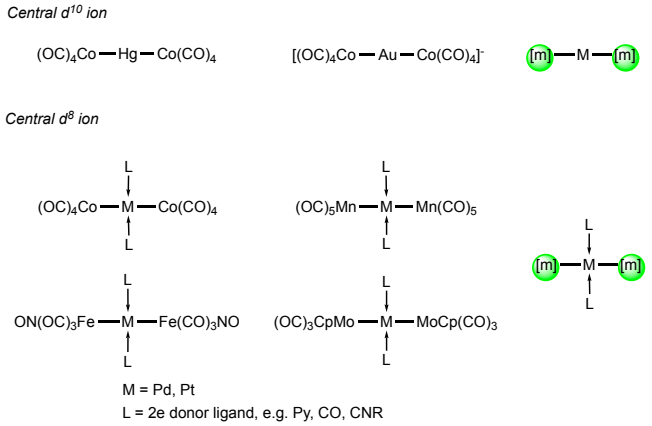


**Figure 1.** Examples of metal carbonyl moieties [m] behaving as terminal "pseudo-halides".

In contrast to the commonly observed terminal bonding mode of the metalloligands [m] mentioned above, an unprecedented situation was observed in a series of centrosymmetric, heterotetranuclear clusters of general formula $\{M_2[m]_2(PR_3)_2\}$ (M = Pd, Pt; [m] = $CrCp(CO)_3$, $MoCp(CO)_3$, $WCp(CO)_3$) (**A**, Figure 2) in which the metalloligand *bridges* a M–M metal-metal bond by formation of two M–[m] metal-metal bonds and semi-doubly and -triply bridging carbonyl ligands.[23-26] The composition of these planar butterfly clusters contrasts with that of hundreds of metal clusters containing a metal carbonyl fragment with one less CO ligand, e.g. $CrCp(CO)_2$, $MoCp(CO)_2$, or $WCp(CO)_2$, which readily satisfy common electron-counting rules.[27,28] Not unexpectedly for clusters containing metals that tend to prefer a 16e over a 18e configuration, these 58e clusters $\{M_2[m]_2(PR_3)_2\}$ do not follow the classical Wade-Mingos rules which associate a butterfly structure with a 62e count,[1] and a localized electron count fails to account for the formation of 5 metal-metal bonds.[29] Even the useful extensions of these rules by Mingos to palladium or platinum clusters[30,31] have limitations since these metals can accommodate either a 16e or a 18e count, which is not always predictable. But if one considers in clusters of type **A** (Figure 2) the whole 18e carbonylmetallate $[m]^-$ as bridging the $d^9$–$d^9$ M–M bond, via direct metal-metal and metal-carbonyl bonding interactions, the structure of these clusters can be readily explained, at least in a qualitative manner. Indeed, an obvious parallel appears between these clusters and dinuclear $Pt^I$ or $Pd^I$ complexes in which the central, dicationic $\{L–M–M–L\}^{2+}$ moiety is bridged by two typical 4e donor monoanionic ligands, such as $(\mu\text{-}PPh_2)^-$ in $[Pt_2(\mu\text{-}PPh_2)_2(PPh_3)_2]$,[32-35] or $(\mu\text{-allyl})^-$ in $[Pd_2(\mu\text{-allyl})_2(PR_3)_2]$ or $[PdPt(\mu\text{-allyl})_2(PR_3)_2]$.[36,37] Each metal centre M in these complexes and in the clusters $\{M_2[m]_2(PR_3)_2\}$ (**A**) reaches a typical and most commonly encountered 16e count when each moiety $[m]^-$ bridging the $d^9$–$d^9$ M–M bond is formally considered as a 4e donor, like e.g. a $(\mu\text{-}PPh_2)^-$ group. The striking bonding similarities between bridging 18e carbonylmetallates and monoanionic bridging ligands, such as halido, phosphanido or allyl donor ligands, are further illustrated in dinuclear $d^9$–$d^9$ complexes where both types of bridging ligands are simultaneously present, a carbonylmetallate and a halide, as in $[Pd_2(\mu\text{-}[m])(\mu\text{-}Cl)(PR_3)_2]$ (**B**, Figure 2),[38] a carbonylmetallate and an allyl ligand, as in $[Pd_2(\mu\text{-}[m])(\mu\text{-allyl})(PR_3)_2]$ (**C**, Figure 2),[39,40] or a carbonylmetallate and a phosphanido ligand, as in $[Pt_2(\mu\text{-}[m])(\mu\text{-}PPh_2)(PPh_3)_2]$[41] (**D**, Figure 2). It is noteworthy that triangular $M'Pd_2$ clusters of type **C** or with a bridging cyclopentadienyl ligand in place of the bridging allyl were precisely prepared by substitution of a bridging 4e donor carboxylate ligand in the dipalladium precursor with the corresponding carbonylmetallate, thus illustrating the synthetic utility of the approach detailed in this paper.[39,40] We wondered whether these bonding similarities could be generalized and allow to readily rationalize the structure of unusual heterometallic clusters containing 16e group 10 metals, in a manner similar to that based on isolobal analogies.[42,43]

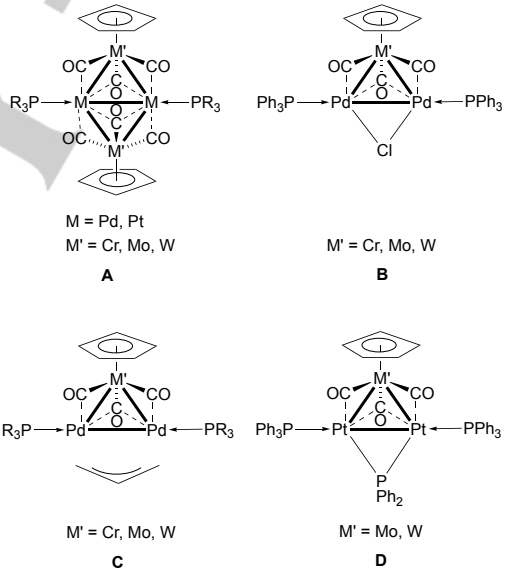


**Figure 2**. Group 6 metals carbonylmetallates $[m]^-$ behaving as bridging 4e donors in clusters containing Group 10 metals.

Other carbonylmetallates than those of the Group 6 metals can experience similar bonding situations. Thus, in previous studies on heterotrinuclear $CoPt_2$ clusters in which the Pt–Pt bond is bridged by a $PPh_2$ group and a $Co(CO)_3L$ moiety (L = $PPh_3$ in $[CoPt_2(\mu\text{-}PPh_2)(CO)_3(PPh_3)_3]$ (**E**, Figure 3),[44] L = CO in $[CoPt_2(\mu\text{-}PPh_2)(CO)_4(PPh_3)_2]$ (**F**),[45] Figure 3), two experimentally observed coordination geometries about the cobalt centre were considered in a comparative Extended Hückel molecular orbital bonding analysis.[45] The distorted trigonal pyramidal (**G**) and tetrahedral arrangements (**H**) (Figure 3) observed in these clusters derive from those encountered for terminally-bound $Co(CO)_3L$ fragments (L = CO, $PPh_3$) in **I** and **J** (Figure 3), respectively. The steric

10.1002/chem.202203557




influence of the $PPh_3$ ligand was less pronounced than expected, indicating the significance of electronic effects in structures of type **G** and **H**. The bonding analysis was consistent with the description of the 18e carbonylmetallates $[Co(CO)_3L]^-$ (L = CO, $PPh_3$) acting as 4e donors, like $PPh_2^-$, bridging a $d^9$–$d^9$ $Pt^I$–$Pt^I$ metal−metal bond where each Pt centre reaches its usual 16e count. This approach nicely applies to other $CoPd_2$ triangular clusters containing a $Co(CO)_4$ moiety in bridging position between two mutually bonded Pd atoms.[38]

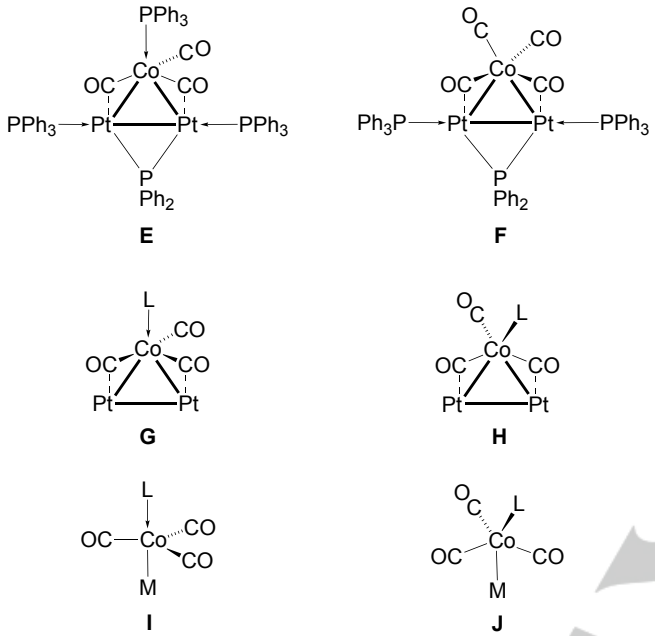


**Figure 3**. Coordination geometries about the cobalt centre when the fragment $Co(CO)_3L$ (L = CO, $PPh_3$) interacts with *two* metal centres (M = Pd, Pt). The distorted trigonal pyramidal (**E**, **G**) and tetrahedral (**F**, **H**) coordination geometries at Co are reminiscent of those encountered when the metalloligand is *terminally* bound to M (**I** and **J**, respectively).

The electronically saturated monoanionic bridging carbonylmetallates and the common bridging ligands mentioned above all interact via their frontier orbitals of suitable symmetry with the acceptor frontier orbitals of *a'* and *a''* symmetry of the monocationic, acceptor moiety $[M_2(\mu\text{-}X)(PR_3)_2]^+$ (Figure 4). These aspects will be detailed below and we will also see that the orientation of the carbonylmetallate donor can adapt to the nature of the acceptor unit to which it is bonded and consequently vary its formal electron donicity.

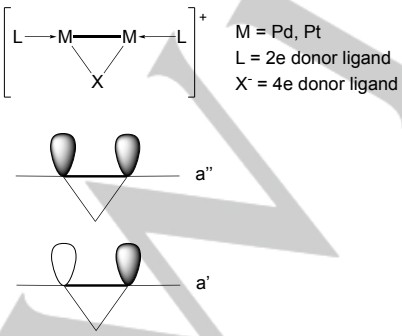


**Figure 4**. Two suitable vacant orbitals to accept electron donation from a 4e donor bridging unit.

From the above qualitative considerations, it appears conceptually attractive to consider that an 18e carbonylmetallate behaves indeed as a "pseudo-halide" and can accordingly act as a terminal (in most cases) or as a bridging metalloligand (rarer). A remarkable extension of this analogy was provided with the first example of structurally characterized metal cluster containing a *triply-bridging* 18e carbonylmetallate (**K**, Figure 5). In this monocationic cluster, three 16e $Pd^{II}$ centres, each chelated by a cyclometallated 8-mq (8-mq-H = 8-methylquinoline) ligand, are triply-bridged on one side of their mean plane by a chlorido ligand and, on the other side, a $MoCp(CO)_3$ moiety.[46] This structural arrangement emphasizes the similarity between these two anionic bridging groups in terms of each donating formally 6e to the 3 $Pd^{II}$ centres. This unique situation will be further discussed below.

The bonding versatility of the carbonylmetallates, potential donors of 2, 4 or 6 electrons, triggered our interest for a deeper bonding analysis that could allow a generalization of the fragment analysis connecting a number of seemingly unrelated metal complexes and clusters. The simplicity of the approach also entails a predicting power with high synthetic potential. Our computational analysis is based on density functional theory (DFT) calculations at the BP86/TZ2P level and carried out with the ADF2000 program (see Computational Details in the SI).[47,48] We will begin by analyzing simple cases, even hypothetical molecules, in order to provide a basis for comparison with more complex situations.

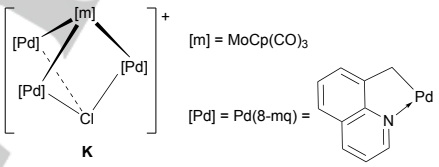


**Figure 5**. In the cluster $[\{Pd(8\text{-}mq)\}_3\{\mu_3\text{-}MoCp(CO)_3\}(\mu_3\text{-}Cl)]^+$, each *triply-bridging* anionic units each behaves as a 6e donor.

Considering a $[M_xXL_n]$ (X = Cl, $Co(CO)_4$, $MoCp(CO)_3$) complex in a given geometry, the ADF program allows a detailed analysis of the interactions between its constituting X and $M_xL_n$ fragments, through a fragment bond energy decomposition analysis (EDA)[49-53] and to express the Kohn-Sham orbitals as linear combinations of the orbitals of the two fragments. The EDA analysis allows to express the total bonding energy between two fragments as the sum of three components: $TBE = E_{Pauli} + E_{Elec} + E_{Orb}$, describing the Pauli repulsion, the electrostatic interaction and the orbital (covalent) interaction, respectively (see Computational Details in the SI). For the sake of simplicity and consistency, we chose to consider the $X^-$ fragment to be a 2, 4 or 6e donor, depending on its coordination mode, *i.e.*, to be a closed-shell anionic ligand ($Cl^-$, $[Co(CO)_4]^-$ and $[MoCp(CO)_3]^-$). The assumed negative charge is purely formal, but allows an easy comparison between the bonding abilities of the various X fragments.

## 2 Results and Discussion

### 2.1 Terminal bonding mode of the metalloligand

We begin our analysis by looking at the bonding between X (X = Cl, $Co(CO)_4$, $MoCp(CO)_3$) and a $Pd^0$ metal centre in a very simple, hypothetical model, namely the linear 14e $[PdX(PH_3)]^-$ complexes (Figure 6). Relevant computed data are given in Table 1. As indicated above, X is assumed to be formally anionic so that the two fragments to be considered are $[Pd(PH_3)]$ and $X^-$.

**Table 1**. Relevant computed data for the model complexes $[PdX(PH_3)]^-$ (X = Cl, $Co(CO)_4$, $MoCp(CO)_3$). All energies are in eV.

| | $[PdCl(PH_3)]^-$ | | $[Pd\{Co(CO)_4\}(PH_3)]^-$ | | $[Pd\{MoCp(CO)_3\}(PH_3)]^-$ | |
|---|---|---|---|---|---|---|
| ***Symmetry*** | $C_{3v}$ | | $C_s$ | | $C_s$ | |
| **HOMO-LUMO gap** | 2.64 | | 2.53 | | 2.79 | |
| **Fragments** | $Pd(PH_3) + Cl^-$ | | $Pd(PH_3) + [Co(CO)_4]^-$ | | $Pd(PH_3)+ [MoCp(CO)_3]^-$ | |
| $E_{Pauli}$ | 2.63 | | 5.53 | | 5.82 | |
| $E_{Elec}$ | -3.13 | | -4.80 | | -5.06 | |
| ***$E_{Orb}$ symmetry components*** | $a_1$<br>$e$ | -0.77<br>-0.53 | $a'$<br>$a''$ | -1.86<br>-0.36 | $a'$<br>$a''$ | -1.42<br>-0.89 |
| $E_{Orb}$ | -1.30 | | -2.22 | | -2.31 | |
| **TBE** | -1.80 | | -1.49 | | -1.55 | |
| **$X^-$ frontier orbital occupation** | $3p_\sigma(a_1)$<br>$3p_\pi$ ($e$) | 1.82<br>2 x 1.93 | $\sigma$ ($a'$)<br>$\pi_\perp$ ($a''$)<br>$\pi_{//}$ ($a'$) | 1.84 + 1.95<br>1.94<br>1.96 | $\sigma$ ($a'$)<br>$\pi_\perp$ ($a''$)<br>$\pi_{//}$ ($a'$) | 1.72 + 1.96<br>1.97<br>1.98 |

It appears from Table 1 that the three $X^-$ moieties present total bonding energies (TBEs) of the same order of magnitude, with chloride displaying a somewhat stronger bonding to the metal. Looking in more details at the three TBE components, one can see that they are significantly larger in absolute value in the case of the two organometallic fragments. In particular, the latter are more covalently bonded to Pd than chloride (compare the $E_{Orb}$ values). Considering first the more symmetrical $[PdCl(PH_3)]^-$ model, it appears that chloride acts not only as a σ-donor ($a_1$ symmetry), but also as a π-donor ligand ($e$ symmetry), the π component representing *ca.* 40% of $E_{Orb}$. This significant π-donating effect is not surprising in view of the presence of $4p_\pi$ accepting atomic orbitals (AOs) on Pd. It can also be traced from the populations of the chloride 3p AOs in the complex (the 3s AO of Cl are not significantly involved in the interaction). They provide an electron transfer of 2 x 0.07 π electron to the metal, whereas the σ donation amounts to 0.18e.

Considering now the Co- and Mo-containing species, we note that the structure of the respective $[Co(CO)_4]^-$ and $[MoCp(CO)_3]^-$ fragments has roughly retained that adopted by the free 18e carbonylmetallates, *i.e.* tetrahedral and pseudo-octahedral, respectively. The occupied d-type level orderings of these anions are sketched in Figure 7.[54] The major donor orbitals of $[Co(CO)_4]^-$ (σ, $\pi_{//}$ and $\pi_\perp$) belong to the $t_2$ set. Note that the orbital labelled σ, which is actually of local δ-type symmetry in Figure 7, gains substantial 4p σ-type hybridization character in the $C_{2v}$-distorted $Co(CO)_4$ fragment of $[Pd\{Co(CO)_4\}(PH_3)]^-$, due to the opening of the in-plane OC–Co–CO angle (115°). The more contracted σ' orbital from the $e$ set is also susceptible to participate in the bonding interactions, but to a lesser extent. The donor orbitals of $[MoCp(CO)_3]^-$ (σ, $\pi_{//}$ and $\pi_\perp$) are the "$t_{2g}$" components of this pseudo-$O_h$ unit.

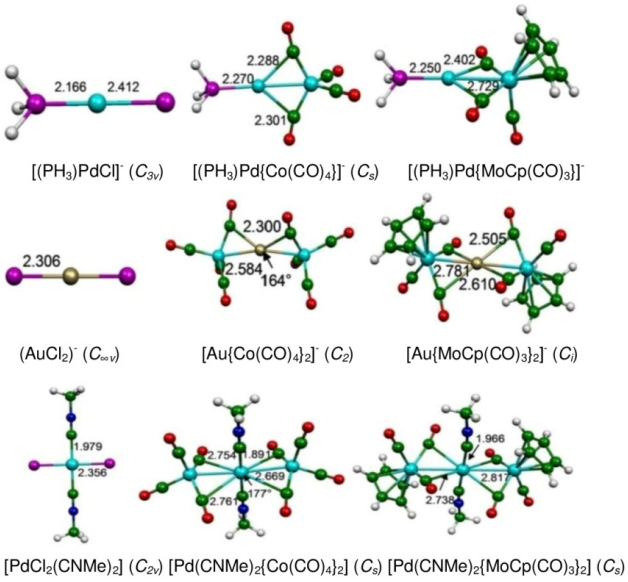


**Figure 6.** Optimized structures of: Top: $[PdX(PH_3)]^-$; middle: $[AuX_2]^-$ and bottom: *trans*-$[PdX_2(CNMe)_2]$ (X = Cl, $Co(CO)_4$, $MoCp(CO)_3$). Distances are given in Å.

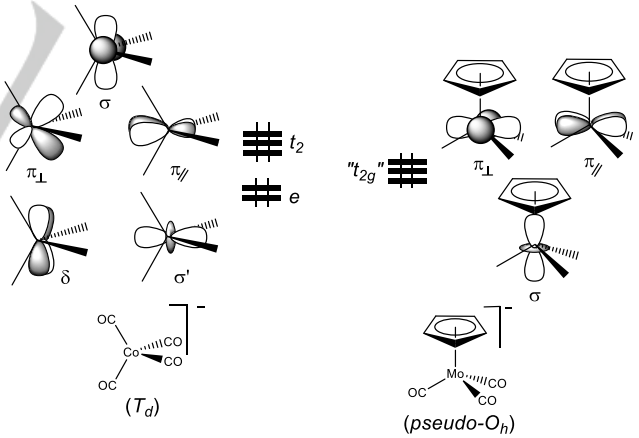


**Figure 7**. Level ordering of the occupied d-type orbitals in the anions $[Co(CO)_4]^-$ and $[MoCp(CO)_3]^-$. In the $C_{2v}$-distorted $Co(CO)_4$ fragment of $[Pd\{Co(CO)_4\}(PH_3)]^-$, the σ labelled orbital is substantially 4p(σ) hybridized (not considered here).

Since both $[Pd\{Co(CO)_4\}(PH_3)]^-$ and $[Pd\{MoCp(CO)_3\}(PH_3)]^-$ have $C_s$ symmetry, it is not possible to separate the σ from the $\pi_{//}$ energy contributions, which belong to the same *a'* representation. However, the σ/π effects can be estimated from the $X^-$ frontier orbital populations, which indicate that the $[Co(CO)_4]^-$ and $[MoCp(CO)_3]^-$ fragments behave rather similarly to chloride, with an even lower π-type electron transfer and, in the case of the Mo-fragment, a larger σ-type electron transfer.

10.1002/chem.202203557




It is important to note that, unlike halides, metal-carbonyl metalloligands can develop, in addition to direct metal-metal bonding, bridging or semi-bridging bonding interactions between their carbonyl ligands and an adjacent metal. Such features are present in both $[Pd\{Co(CO)_4\}(PH_3)]^-$ and $[Pd\{MoCp(CO)_3\}(PH_3)]^-$ models (Figure 6) and originate from electron donation from occupied 4d-type Pd orbitals into vacant $\pi^*(CO)$ orbitals of the metalloligand. In both Co and Mo models, this electron donation involves mainly the $\pi_{//}$ component of the 4d(Pd) shell and the LUMO of the organometallic fragment, which is an antisymmetrical combination of "in-plane" $\pi^*(CO)$ orbitals. The occupation of this fragment orbital is 0.16e in both complexes. The resulting bonding combination of these two fragment orbitals in $[Pd\{Co(CO)_4\}(PH_3)]^-$ and $[Pd\{MoCp(CO)_3\}(PH_3)]^-$ is plotted in Figure 8. This secondary but non-negligible bonding interaction adds to the major bonding that results from direct $X^- \rightarrow Pd$ bonding.

Even though the monosubstituted models $[PdX(PR_3)]^-$ (X = Cl, $Co(CO)_4$, $MoCp(CO)_3$) were hypothetical, the related isoelectronic series $[AuX_2]^-$ (X = halide, $Co(CO)_4$ or $MoCp(CO)_3$) is known, and the structures of the linear, disubstituted Au(I) complexes $[AuX_2]^-$ (X = Cl, Br, I),[55] $[Au\{CrCp(CO)_3\}_2]^-$,[13] and $[Au\{MoCp(CO)_3\}_2]^-$ have been determined by X-ray diffraction.[14] Our calculations resulted in the optimized geometries shown in Figure 6. That of $[Au\{MoCp(CO)_3\}_2]^-$ is in very good agreement with the experimental structure.[14] The computed EDA data, based on the [AuX] + $X^-$ fragmentation, are given in the Supporting Information (Table S1). Because the central metal is different, the energy terms differ from those of Table 1, but they follow the same trend within the series. The occupation of the $X^-$ frontier orbitals is close to that in Table 1, and the Co and Mo derivatives exhibit similar CO semi-bridging features to their Pd analogues.

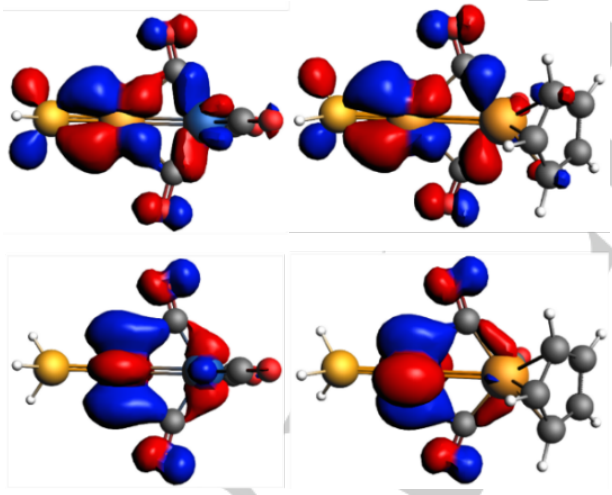

**Figure 8.** Plots of the occupied bonding orbitals of the model systems $[Pd\{Co(CO)_4\}(PH_3)]^-$ (left) and $[Pd\{MoCp(CO)_3\}(PH_3)]^-$ (right) associated with Pd···CO semi-bridging interactions.

A linear X–M–X (M = Pd, Pt) arrangement, where X = $Co(CO)_4$, $MoCp(CO)_3$ or another isolobal metal carbonyl moiety, is also present in several complexes of the type *trans*-$[X–ML_2–X]$ (L = CNR, NCR, CO, pyridine, carbene).[15,16,18-22,26,56,57] For this reason, the *trans*-$[X–Pd(CNMe)_2–X]$ (X = Cl, $Co(CO)_4$, $MoCp(CO)_3$) series was selected and the optimized structures are shown in Figure 6. They all exhibit the square planar coordination geometry expected for a tetracoordinated $Pd^{II}$ ($d^8$) metal centre. The computed EDA data, based on the fragmentation in $[PdX(CNMe)_2]^+ + X^-$ are given in Table S2. The values display similar trends to those found in the two previous series. At this stage of the analysis, it is important to emphasize that, although the variations of TBE within each of the three families of complexes shown in Figure 6 are similar, the three families differ in their TBE magnitude (Tables 1, S1 and S2). These differences originate to a large extent from their $E_{Pauli}$ and $E_{Elec}$ components, which strongly depend on the nature and charge of the Pd/Au organometallic fragment with which $X^-$ interacts. The $E_{Orb}$ component is less affected, likewise the occupation of the $X^-$ frontier orbitals. These covalency descriptors are consistent with a predominantly σ bonding character (as expected for a terminal bonding mode), which, in the case of the two metalloligands, is stronger than or similar to that displayed when $X^-$ = chloride. In these situations, the metalloligands develop additional bonding with the metal they are attached to through semi-bridging CO interactions.

### 2.2 Doubly bridging bonding mode $\mu_2$ of the metalloligand

As mentioned in the Introduction, the metalloligands X = $Co(CO)_4$ and $MoCp(CO)_3$ are able to bridge a covalent metal-metal bonds, as observed in heterometallic clusters containing a Pd–Pd or a Pt–Pt unit, such as those mentioned in the Introduction (**A**–**F**, Figures 2 and 3).[23-26,29,41,44,45,58,59] The three resulting metal-metal bonds allow the metal centres to reach a stable 18e (Co, Mo) or 16e (Pd, Pt) electron count. To mimic this structural chemistry, we first designed the simplified model series $[Pd_2(\mu\text{-}PH_2)(\mu\text{-}X)(PH_3)_2]$ in which X bridges a Pd–Pd single bond. The optimized geometries are shown at the top of Figure 9 and selected computed data are given in Table 2. We first address the question of the stereochemical environment of the Co atom in the family of clusters $[M_2(\mu\text{-}PR_2)\{\mu\text{-}Co(CO)_3L\}(PR'_3)_2]$ (M = Pd, Pt; L = CO, $PR_3$).[44,45] As mentioned above, the Co atom in these compounds has a 18e environment. Although hexacoordinated 18e metal centres tend to adopt an octahedral coordination sphere, the μ-$Co(CO)_4$ fragment in these compounds does not exhibit the expected $C_{2v}$ local symmetry of an octahedral moiety from which two proximal bonds have been removed. The frontier orbitals of an octahedron-derived $C_{2v}$-type $[Co(CO)_4]^-$ unit are sketched on the left side of Figure 10.[42,54] The two orbitals used for completing the octahedral coordination sphere of Co are the hybrids labelled σ and $\pi_{//}$. The corresponding optimized geometry, of $C_{2v}$ symmetry, is shown in Figure 11 (left). It exhibits a substantial distortion away from ideal linearity of the axial OC–Co–CO angle (130 °) with two carbonyl ligands bending towards the Pd atoms, in search of OC···Pd interactions (C···Pd = 2.64 Å). In this structure, the environment around the Co centre is best viewed as forming a distorted tetrahedron rather than derived from an octahedron, as sketched on the left side of Figure 10. Rotating this $Co(CO)_4$ unit by 180° brings the "axial" carbonyls in the $CoPd_2$ plane, thus closer to the Pd centres. In the resulting optimized $C_{2v}$ structure (Figure 9, middle), Co is no longer octahedrally coordinated, but the local $Co(CO)_4$ stereochemistry now resembles that on the left side of Figure 10 (rotated by 180°), which allows the use of less suitable $\pi_\perp$ frontier orbital (together with the hybrid σ) for bonding with the Pd atoms. Whereas the Co–Pd bond is weaker, the OC···Pd bridging interactions are

stronger (C···Pd = 2.23 Å). Interestingly, this $C_{2v}$ structure is not an energy minimum and, when symmetry constraints are released, it evolves towards the structure of $C_s$ symmetry that is shown on the right side of Figure 10. This energy minimum geometry is similar to the experimental structure of $[M_2(\mu\text{-}PPh_2)\{\mu\text{-}Co(CO)_4\}(PPh_3)_2]$ (M = Pt, Pd).[45] It exhibits a $Co(CO)_4$ unit that can be locally described as a distorted tetrahedron,[44,45] and which maximizes OC···Pd (2.26 Å) bonding while keeping strong Co–Pd bonds (2.67 Å). Interestingly, in the X-ray structure of $[Pt_2(\mu\text{-}PPh_2)\{\mu\text{-}Co(CO)_3(PPh_3)\}(PR'_3)_2]$,[44] the $Co(CO)_3(PPh_3)$ fragment adopts a conformation slightly closer to that of a trigonal pyramid, similar to the ideal one sketched on the right side of Figure 10. However, our optimized structure of the model $[Pd_2(\mu\text{-}PH_2)\{\mu\text{-}Co(CO)_3(PH_3)\}(PH_3)_2]$ does not reproduce this trend, for it is very similar to that of $[Pd_2(\mu\text{-}PH_2)\{\mu\text{-}Co(CO)_4\}(PH_3)_2]$. In any case, the geometrical differences between the two X-ray structures of $[Pt_2(\mu\text{-}PPh_2)\{\mu\text{-}Co(CO)_3L\}(PPh_3)_2]$ (L = CO, $PPh_3$)[44,45] remain relatively minor. As a whole, these results illustrate the large stereochemical flexibility of the $Co(CO)_4$ fragment, in part due to its capacity to develop CO (semi-)bridging interactions. In the configuration of lowest energy of $[Pd_2(\mu\text{-}PH_2)\{\mu\text{-}Co(CO)_4\}(PH_3)_2]$ (right hand side of Figure 11), two $\pi^*$(CO) combinations are mainly involved in this bonding, receiving a total of 0.21e from the Pd 4d orbitals.

The $Pd_2(\mu\text{-}PH_2)\{\mu\text{-}MoCp(CO)_3\}(PH_3)_2$ model exhibits also bridging COs, involving this time the three carbonyls. The three most important $\pi^*$(CO) combinations of the Mo fragment receive a total of 0.32e. Thus, for this compound, CO bridging is a non-negligible component of $E_{Orb}$ (Table 2). This explains in part why $E_{Orb}$ is substantially smaller in the case of chlorine and larger in the case of the Mo model.

Nevertheless, when looking at the occupations of the $X^-$ frontier orbital (Table 2), rather similar values are found for the three fragments, indicating similar bonding abilities when CO bridging is not considered.

**Figure 9.** Optimized structures of: Top: $Pd_2(\mu\text{-}PH_2)X[(PH_3)_2]$; middle: $Pd_2(PH_3)_2(\mu\text{-}X)_2$; bottom: $[Ag_4\{Co(CO)_4\}_3X]$ (X = Cl, $Co(CO)_4$ and $MoCp(CO)_3$). Distances are given in Å.

Next, we considered the situation where the Pd–Pd bond is doubly bridged by X = Cl, $Co(CO)_4$ or $MoCp(CO)_3$, and investigated the $Pd_2(PH_3)_2(\mu\text{-}X)_2$ model series. Related isoelectronic, centrosymmetric platinum-containing $[Pt_2\{\mu\text{-}MCp(CO)_3\}_2(PR_3)_2]$ (M = Mo, W) clusters are well documented (**A**, Figure 2)[24,26] and can be handled in the same way as their Pd analogs. The optimized $Pd_2X_2$ planar triangulated rhombohedral geometries are shown in the middle of Figure 9 and computed data are given in Table S3. Unsurprisingly, they exhibit similar connectivities to their monosubstituted homologues (top of Figure 9), indicating similar bonding modes. The model corresponding to X = $MoCp(CO)_3$ is fully consistent with the structures of the planar forms of $[Pd_2\{\mu\text{-}MCp(CO)_3\}_2(PR_3)_2]$ (M = Cr, Mo, W) determined by X-ray diffraction.[23,25] Replacing $\mu$-$PH_2$ by $\mu$-X results for the di-substituted species in a slight shortening of the Pd–Pd and Pd–X distances compared to those of the monosubstituted ones. Consistently, the various components of the total bonding energy between the $X^-$ and $[Pd_2(PH_3)_2(\mu\text{-}X)]^+$ fragments differ somewhat. In particular, the $E_{orb}$ components indicate stronger covalency in the di-substituted species (-3.90, -5.39 and -5.91 eV for X = Cl, $Co(CO)_4$ and $MoCp(CO)_3$, respectively).

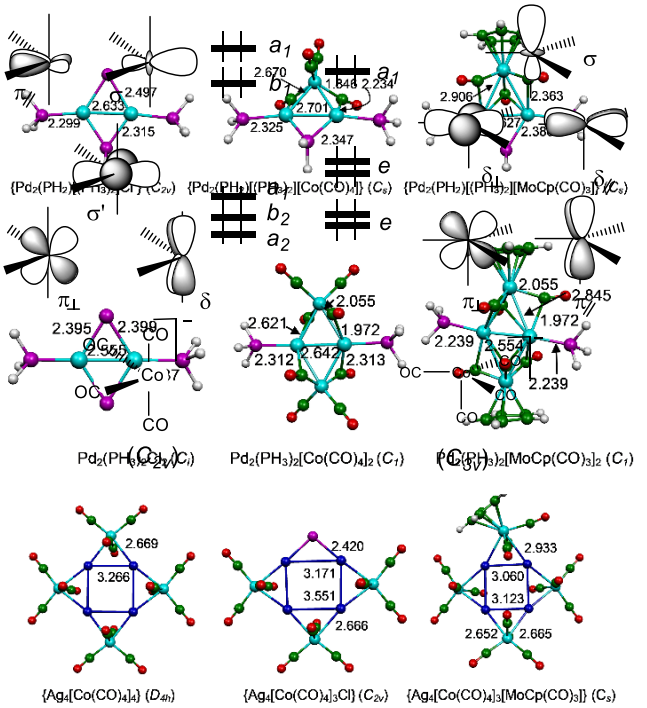


**Figure 10**. Level ordering of the occupied d-type orbitals of a $[Co(CO)_4]^-$ fragment in two different geometries. Left: Octahedron-derived. Right: Trigonal pyramidal-derived.



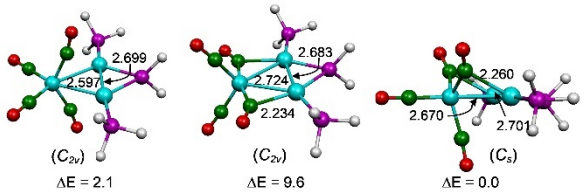


**Figure 11.** Optimized geometries of $Pd_2(\mu\text{-}PH_2)\{\mu\text{-}Co(CO)_4\}(PH_3)_2$ assuming various symmetry constraints. Relative energies are given in kcal/mol. The global energy minimum, of $C_s$ symmetry, corresponds to **E,** Figure 3.

Whereas in the latter complexes the X = Cl, $Co(CO)_4$ and $MoCp(CO)_3$ units bridge a metal-metal single bond, one may wonder about their behavior when no significant covalent character exists between the two bridged metals, such as in the $d^{10}$ $M^I$ (M = Cu, Ag, Au) triangular $[M_3(\mu\text{-}X)_3]$ or square $[M_4(\mu\text{-}X)_4]$ raft-type structures,[7,60-63] or in their related isoelectronic iron analogues $[M_3\{\mu\text{-}Fe(CO)_4\}_3]^{3-}$ and $[M_4\{\mu\text{-}Fe(CO)_4\}_4]^{4-}$.[64-66] The bonding in these complexes can be simply described as resulting from the donation of two electron pairs by the 18e $\mu$-$[Co(CO)_4]$, $\mu$-$[MoCp(CO)_3]^-$ or $\mu$-$[Fe(CO)_4]^{2-}$ units to each of the $d^{10}$ $M^I$ centres they bridge. As a result, the $M^I$ centres become linearly coordinated by two hetero-metals and reach their usual 14e configuration. Weak additional $d^{10}\cdots d^{10}$ metallophilic interactions between neighboring $d^{10}$ $M^I$ centres increase slightly the stability of these clusters.[7,62,66] Starting from the above-mentioned compounds, the hypothetical series $[Ag_4(\mu\text{-}X)\{\mu\text{-}Co(CO)_4\}_3]$ (X = Cl, $Co(CO)_4$, $MoCp(CO)_3$) was examined. Their optimized geometries (bottom of Figure 9) are consistent with the X-ray structure of the $Ag_4Co_4$ cluster.[61] It is important to note that in these models, the $Co(CO)_4$ fragments have adapted their local

stereochemistry to the bonding requirements of the Ag atoms they are connected to. They adopt now the local octahedron-derived $C_{2v}$ geometry illustrated on the left side of Figure 10. Although the flexibility of the $MoCp(CO)_3$ fragment is more limited, it also tends to somewhat distort away from its pseudo-octahedral environment (Figure 7) to better adapt to the formation of two Mo–Ag localized bonds.

The main computed data for the $[Ag_4(\mu_2\text{-}X)\{\mu_2\text{-}Co(CO)_4\}_3]$ (X = Cl, $Co(CO)_4$, $MoCp(CO)_3$) series are given in Table 3. Unsurprisingly, the bonding is dominated by the in-plane σ-type and $\pi_{//}$-type orbitals, whereas the π-type interactions involving $\pi_\perp$ and its accepting Ag 5p counterpart remain minor. The general trend within the X = $Cl^-$, $[Co(CO)_4]^-$ and $[MoCp(CO)_3]^-$ series is the same as in the complexes of Table 2, in particular the occurrence of a stronger covalent interaction ($E_{Orb}$) in the case of the organometallic fragments, mainly associated with the σ–type component. In this particular series, carbonyl semi-bridging interactions are negligible, due to the poor donor ability of the low-lying 4d(Ag) AOs. As a whole, it is clear that the three $X^-$ units behave similarly with respect to the $Ag^I\cdots Ag^I$ edge they bridge.

**Table 2**. Relevant computed data for the $[Pd_2(\mu\text{-}PH_2)(\mu\text{-}X)(PH_3)_2]$ (X = Cl, $Co(CO)_4$, $MoCp(CO)_3$) series. All energies are in eV.

| | $Pd_2(PH_2)Cl(PH_3)_2$ | | $Pd_2(PH_2)\{Co(CO)_4\}(PH_3)_2$ | | $Pd_2(PH_2)\{MoCp(CO)_3\}(PH_3)_2$ | |
|---|---|---|---|---|---|---|
| ***Symmetry*** | $C_{2v}$ | | $C_s$ | | $C_s$ | |
| **HOMO-LUMO gap** | 1.45 | | 1.22 | | 1.0 | |
| **Fragments** | $[Pd_2(PH_2)(PH_3)_2]^+ + Cl^-$ | | $[Pd_2(PH_2)(PH_3)_2]^+ + [Co(CO)_4]^-$ | | $[Pd_2(PH_2)(PH_3)_2]^+ + [Mo(CO)_3Cp]^-$ | |
| $E_{Pauli}$ | 5.53 | | 9.24 | | 10.55 | |
| $E_{Elec}$ | -8.83 | | -10.97 | | -11.78 | |
| ***$E_{Orb}$ symmetry components*** | $a_1$<br>$a_2$<br>$b_1$<br>$b_2$ | -1.45<br>-0.05<br>-0.28<br>-1.05 | $a'$<br>$a''$ | -2.22<br>-1.76 | $a'$<br>$a''$ | -2.68<br>-2.34 |
| $E_{Orb}$ | -2.83 | | -3.98 | | -5.02 | |
| **TBE** | -6.13 | | -5.72 | | -6.25 | |
| **$X^-$ frontier orbital occupations** | σ ($a_1$)<br>$\pi_{//}$ ($b_2$)<br>$\pi_\perp$ ($b_1$) | 1.75<br>1.70<br>1.92 | σ ($a_1$)<br>$\pi_{//}$ ($a''$)<br>$\pi_\perp$ ($a'$) | 1.72<br>1.74<br>1.93 | σ ($a'$)<br>$\pi_{//}$ ($a''$)<br>$\pi_\perp$ ($a'$) | 1.73<br>1.57<br>1.93 |



**Table 3**. Relevant computed data for the $[Ag_4(\mu\text{-}X)\{\mu\text{-}Co(CO)_4\}_3]$ (X = Cl, $Co(CO)_4$, $MoCp(CO)_3$) series. All energies are in eV. In the case of the cobalt derivative, the EDA is performed within the $C_{2v}$ local fragment symmetries.

| | $[Ag_4\{Co(CO)_4\}_3Cl]$ | | $[Ag_4\{Co(CO)_4\}_4]$ | | $[Ag_4\{Co(CO)_4\}_3\{MoCp(CO)_3\}]$ | |
|---|---|---|---|---|---|---|
| ***Symmetry*** | $C_{2v}$ | | $D_{4h}$ | | $C_1$ | |
| **HOMO-LUMO gap** | 2.98 | | 2.59 | | 2.45 | |
| **Fragments** | $[Ag_4\{Co_3(CO)_4\}_3]^+ + Cl^-$ | | $[Ag_4\{Co_3(CO)_4\}_3]^+ + [Co(CO)_4]^-$ | | $[Ag_4\{Co_3(CO)_4\}_3]^+ + [MoCp(CO)_3]^-$ | |
| $E_{Pauli}$ | 5.13 | | 5.68 | | 6.77 | |
| $E_{Elec}$ | -9.79 | | -8.79 | | -9.63 | |
| ***$E_{Orb}$ symmetry components*** | $a_1$<br>$a_2$<br>$b_1$<br>$b_2$ | -1.47<br>-0.08<br>-0.27<br>-0.92 | $a_1$<br>$a_2$<br>$b_1$<br>$b_2$ | -1.97<br>-0.22<br>-0.37<br>-0.84 | $a$ | -4.23 |
| $E_{Orb}$ | -2.74 | | -3.40 | | -4.23 | |
| **TBE** | -7.40 | | -6.51 | | -7.10 | |
| **$X^-$ frontier orbital occupations** | σ ($a_1$)<br>$\pi_{//}$ ($b_2$)<br>$\pi_\perp$ ($b_1$) | 1.73<br>1.67<br>1.99 | σ ($a_1$)<br>$\pi_{//}$ ($b_2$)<br>$\pi_\perp$ ($b_1$) | 1.43<br>1.72<br>1.97 | σ ($a$)<br>$\pi_{//}$ ($a$)<br>$\pi_\perp$ ($a$) | 1.26<br>1.58<br>1.98 |

### 2.3 Triply bridging bonding mode $\mu_3$ of the metalloligand

As in the case of the edge-bridging $\mu_2$-bonding mode discussed above, we first consider compounds in which $X^-$ is triply bridging a triangular $Pd_3$ face containing three Pd–Pd bonds in the model series $[Pd_3(\mu_3\text{-}X)(CO)_6]^-$ (X = $Cl^-$, $[Co(CO)_4]^-$, $[MoCp(CO)_3]^-$). It turned out that in the molybdenum case, the bonding interaction

between the two fragments was found to be particularly weak, due to steric hindrance. This model was thus discarded in the results provided in Figure 12 (top) and Table 4. The $\mu_3$-$[Co(CO)_4]^-$ unit adopts a trigonal pyramidal local $C_{3v}$ geometry suited for donation of three electron pairs,[54] one of $\sigma$-type and two degenerate $\pi$-type orbitals (right hand side of Figure 10). It displays more covalent character than $Cl^-$ in the interaction with the $Pd_3$ triangle, as evidenced by the $E_{orb}$ components. This is in part due to the existence of three semi-bridging carbonyl ligands of which the major $\pi^*$(CO) combinations receive 0.14e from the 4d Pd(4d) AOs.

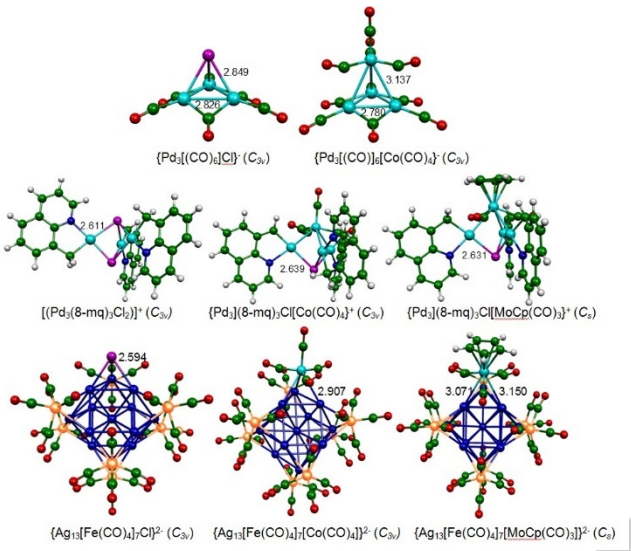


**Figure 12.** Top: Optimized structures of $[Pd_3X(CO)_6]$ (X = Cl and $Co(CO)_4$). Middle: Optimized structures of $[\{Pd(8\text{-mq})\}_3(\mu_3\text{-Cl})(\mu_3\text{-X})]^+$ (X = Cl, $Co(CO)_4$, $MoCp(CO)_3$). Bottom: Optimized structures of $[Ag_{13}\{Fe(CO)_4\}_7X]^{2-}$ (X = Cl, $Co(CO)_4$ and $MoCp(CO)_3$). Distances are given in Å.



As mentioned in the Introduction, a unique example of structurally characterized $\mu_3$-$MoCp(CO)_3$ moiety bridging an open $Pd_3$ triangle (with no significant direct Pd–Pd bonding) has been reported with $[\{Pd(8\text{-mq})\}_3(\mu_3\text{-Cl})\{\mu_3\text{-}MoCp(CO)_3\}]^+$ (8-mq-H = 8-methylquinoline; see Figure 5).[46] The optimized geometry of this cluster (middle right of Figure 12) nicely reproduces the structural data obtained by X-ray diffraction.[46] Replacing in this cluster the fragment $MoCp(CO)_3$ by Cl or $Co(CO)_4$ yielded similar optimized hypothetical architectures (Figure 12, middle). The main computed data for the series $[\{Pd(8\text{-mq})\}_3(\mu_3\text{-Cl})(\mu_3\text{-X})]^+$ (X = Cl, $Co(CO)_4$, $MoCp(CO)_3$) are gathered in Table 5. Again, the three $X^-$ fragments interact similarly with the $Pd_3$ triangle, donating three electron pairs via one $\sigma$- and two $\pi$-type occupied frontier orbitals. As in the previous series, the $E_{Orb}$ values indicate stronger covalent interactions in the case of the organometallic fragments. The difference is however particularly pronounced in this case, in part because of stronger CO semi-bridging interactions. The associated Pd→$\pi^*$(CO) donation is 0.59e and 0.56e in the case of X = $Co(CO)_4$ and $MoCp(CO)_3$, respectively. However, the differences in the TBE values remain moderate. Since in the $[\{Pd(8\text{-mq})\}_3(\mu_3\text{-Cl})(\mu_3\text{-X})]^+$ series, the $\mu_3$-Cl atom and the $\mu_3$-X group interact with the $[Pd_3(8\text{-mq})_3X]^{2+}$ fragment in a similar symmetrical fashion, it is possible to compare the bonding of the isolobal $\mu_3$-Cl and $\mu_3$-X units in the same molecule. The corresponding EDA analysis indicates that in the case of X = $Co(CO)_4$, Cl interacts similarly as in the hypothetical $[Pd_3(8\text{-mq})_3Cl_2]^+$ dichloride. When X = $MoCp(CO)_3$, the chloride donates less 3p($\pi$) electron density, but as a whole, the EDA data remain rather similar in the three compounds.

**Table 4.** Relevant computed data for the $[Pd_3(CO)_6(\mu_3\text{-X})]^-$ (X = Cl, $Co(CO)_4$, $MoCp(CO)_3$) series. All energies are in eV.

| | $[Pd_3(CO)_6(Cl)]^-$ | | $[Pd_3(CO)_6\{Co(CO)_4\}]^-$ | |
|---|---|---|---|---|
| ***Symmetry*** | $C_{3v}$ | | $C_{3v}$ | |
| **HOMO-LUMO gap** | 2.52 | | 2.16 | |
| **Fragments** | $[Pd_3(CO)_6] + Cl^-$ | | $[Pd_3(CO)_6] + [Co(CO)_4]^-$ | |
| $E_{Pauli}$ | 3.76 | | 5.93 | |
| $E_{Elec}$ | -3.70 | | -4.98 | |
| $E_{Orb}$ **symmetry components** | $a_1$<br>$a_2$<br>$e$ | -1.38<br>-0.04<br>-0.68 | $a_1$<br>$a_2$<br>$e$ | -1.52<br>-0.04<br>-0.91 |
| $E_{Orb}$ | -2.08 | | -2.47 | |
| **TBE** | -2.02 | | -1.52 | |
| $X^-$ **frontier orbital occupations** | $\sigma$ ($a_1$)<br>$\pi$ ($e$) | 1.70<br>2 x 1.88 | $\sigma$ ($a_1$)<br>$\pi$ ($e$) | 1.51<br>2 x 1.96 |

As we did in the case of the edge-bridging $\mu_2$-bonding mode of the organometallic fragment discussed above, let us now consider their $\mu_3$-bridging to $d^{10}$ $M^I$ metal centres in systems with no covalent M–M bond. To our knowledge, there is no example with a $Co(CO)_4$ or $MoCp(CO)_3$ unit triply bridging such a triangular face, but an $Fe(CO)_4$ analog exists in $[Ag_{12}(\mu_{12}\text{-Ag})\{\mu_3\text{-}Fe(CO)_4\}_8]^{n-}$ (n = 3-5).[67,68] This cluster displays a centered cuboctahedral core of silver atoms, the eight triangular faces of which are capped by $Fe(CO)_4$ units. Its trianionic form can be simply described as made of $d^{10}$ $Ag^I$ centres, twelve of them being in an approximate linear coordination mode, receiving two electron pairs from two formally $[Fe(CO)_4]^{2-}$ units and therefore reaching the stable 14e configuration. The bonding between the central $Ag^I$ ion and the $Ag_{12}$ icosahedral cage is mainly ionic, with additional 4d/5s covalent interactions.[69] The $\mu_3$-$[Fe(CO)_4]^{2-}$ units adopt the trigonal pyramidal local coordination geometry suited for the donation of three electron pairs,[54] (analogous to $Co(CO)_4^-$ on the right hand side of Figure 10). We therefore designed a model series in which one of the $[Fe(CO)_4]^{2-}$ unit from the above trianion is replaced by an isoelectronic $X^-$ = $Cl^-$, $[Co(CO)_4]^-$ or $[MoCp(CO)_3]^-$ group. The optimized geometries of the resulting $[Ag_{12}(\mu_{12}\text{-Ag})\{\mu_3\text{-}Fe(CO)_4\}_7(\mu_3\text{-X})]^{2-}$ clusters are shown in Figure 12 (bottom line) and the main computed data are given in Table 6. They indicate that, once again, the molybdenum unit is more covalently bonded than the other two fragments.

**Table 5.** Relevant computed data for the $[\{Pd(8\text{-mq})\}_3(\mu_3\text{-Cl})(\mu_3\text{-X})]^+$ (X = Cl, $Co(CO)_4$, $MoCp(CO)_3$) series. All energies are in eV.

| | $[Pd_3(8\text{-mq})_3Cl_2]^+$ | $[Pd_3(8\text{-mq})_3Cl\{Co(CO)_4\}]^+$ | | $[Pd_3(8\text{-mq})_3Cl\{MoCp(CO)_3\}]^+$ | |
|---|---|---|---|---|---|
| ***Symmetry*** | $C_{3v}$ | $C_{3v}$ | | $C_s$ | |
| **HOMO-LUMO gap** | 2.44 | 2.15 | | 1.93 | |
| **Fragments** | $[Pd_3(8\text{-mq})_3Cl]^{2+}$ + $Cl^-$ | $[Pd_3(8\text{-mq})_3Cl]^{2+}$ + $[Co(CO)_4]^-$ | $[Pd_3(8\text{-mq})_3\{Co(CO)_4\}]^{2+}$ + $Cl^-$ | $[Pd_3(8\text{-mq})_3Cl]^{2+}$ + $[MoCp(CO)_3]^-$ | $[Pd_3(8\text{-mq})_3\{MoCp(CO)_3\}]^{2+}$ + $Cl^-$ |
| $E_{Pauli}$ | 6.23 | 18.32 | 7.13 | 19.95 | 6.69 |
| $E_{Elec}$ | -11.88 | -19.48 | -12.49 | -21.04 | -11.26 |
| ***$E_{Orb}$ symmetry components*** | *$a_1$* *-1.36*<br>*$a_2$* *-0.09*<br>*e* *-1.63* | *$a_1$* *-1.88*<br>*$a_2$* *-0.96*<br>*e* *-5.61* | *$a_1$* *-1.62*<br>*$a_2$* *-0.08*<br>*e* *-1.69* | *a'* *-5.34*<br>*a"* *-4.30* | *a'* *-2.85*<br>*a"* *-0.75* |
| $E_{Orb}$ | -3.08 | -8.45 | -3.39 | -9.64 | -3.60 |
| **TBE** | -8.73 | -9.61 | -8.75 | -10.73 | -8.17 |
| **$X^-$ frontier orbital occupations** | $\sigma$ ($a_1$) 1.76<br>$\pi$ (e) 2 x 1.78 | $\sigma$ ($a_1$) 1.74<br>$\pi$ (e) 2 x 1.74 | $\sigma$ ($a_1$) 1.75<br>$\pi$ (e) 2 x 1.77 | $\sigma$(*a'*) 1.47 + 1.85<br>$\pi_{//}$ (*a"*) 1.47<br>$\pi_{\perp}$ (*a'*) 1.67 | $\sigma$(*a'*) 1.72 + 1.78<br>$\pi_{//}$ (*a"*) 1.81<br>$\pi_{\perp}$ (*a'*)1.97 |

**Table 6.** Relevant computed data for the $[Ag_{12}(\mu_{12}\text{-Ag})\{\mu_3\text{-Fe}(CO)_4\}_7(\mu_3\text{-X})]^{2-}$ (X = Cl, $Co(CO)_4$, $MoCp(CO)_3$) series. All energies are in eV.

| | $[Ag_{13}\{Fe(CO)_4\}_7Cl]^{2-}$ | $[Ag_{13}\{Fe(CO)_4\}_7\{Co(CO)_4\}]^{2-}$ | $[Ag_{13}\{Fe(CO)_4\}_7\{MoCp(CO)_3\}]^{2-}$ |
|---|---|---|---|
| ***Symmetry*** | $C_{3v}$ | $C_{3v}$ | $C_s$ |
| **HOMO-LUMO gap** | 0.68 | 0.64 | 0.70 |
| **Fragments** | $[Ag_{13}\{Fe(CO)_4\}_7]^-$ + $Cl^-$ | $[Ag_{13}\{Fe(CO)_4\}_7]^-$ + $[Co(CO)_4]^-$ | $[Ag_{13}\{Fe(CO)_4\}_7]^-$ + $[MoCp(CO)_3]^-$ |
| $E_{Pauli}$ | 7.33 | 7.51 | 10.85 |
| $E_{Elec}$ | -6.26 | -5.34 | -7.83 |
| ***$E_{Orb}$ symmetry components*** | *$a_1$* -2.53<br>*$a_2$* -0.03<br>*e* -1.22 | *$a_1$* -2.57<br>*$a_2$* -0.11<br>*e* -1.25 | *a'* -3.81<br>*a"* -1.33 |
| $E_{Orb}$ | -3.78 | -3.93 | -5.14 |
| **TBE** | -2.71 | -1.76 | -2.12 |
| **$X^-$ frontier orbital occupations** | $\sigma$ ($a_1$) 1.65<br>$\pi$ (e) 2 x 1.84 | $\sigma$ ($a_1$) 1.33<br>$\pi$ (e) 2 x 1.90 | $\sigma$ (*a'*) 1.43<br>$\pi_{//}$ (*a'*) 1.65<br>$\pi_{\perp}$ (*a"*) 1.82 |



## Conclusion

We have shown that 18e organometallic fragments such as $[Co(CO)_4]^-$, $[MoCp(CO)_3]^-$ or $[Fe(CO)_4]^{2-}$ can behave as versatile terminal, doubly- or triply-bridging metalloligands in metal-metal bonded complexes and clusters through formal donation of 2-, 4- or 6e, in the same way as 8e halides and chalcogenides. Whereas the main-group anions have their three frontier orbitals always "prepared" for building one, two or three bonds with metal centres, this is not the case of the organometallic fragments, because their bonding abilities depend strongly on their spatial configuration. However, the isolobal analogy between the two types of ligands is always rendered possible due to the large structural flexibility of the organometallic unit, which can adapt to the electron acceptor unit. Thus for example, the fragment $[Co(CO)_4]$ can vary its local

structure to provide the suitable set of frontier orbitals ideally prepared for terminal, $\mu_2$ or $\mu_3$ bridging modes (Figures 7 and 11). In the case of $[MoCp(CO)_3]$, an opening of the $Mo(CO)_3$ cone is observed, when compared with the uncoordinated anion $[MoCp(CO)_3]^-$,[70,71] upon interaction of the metalloligand with two or three metal centres, allowing a rather symmetrical capping by two or three metal-metal bonds, respectively. When compared to chloride, the metalloligands display stronger orbital interactions in the ligand-to-metal bonding. They also possess the unique ability to develop CO (semi)-bridging interactions with the metals they are connected to in addition to the direct metal-metal interaction(s). When structurally and electronically allowed, the contribution of these additional interactions involving back-bonding into the $\pi^*$(CO) orbitals should not be overlooked. Considering the bonding analogy between electronically saturated halides, or other ubiquitous ligands mentioned in the Introduction (e.g. phosphido, allyl ligands) and metalloligands viewed as "pseudo-halides" greatly facilitates electron bookkeeping in metal carbonyl clusters that are not readily amenable to usual electron-counting procedures. The considerations detailed in this work for $[Co(CO)_4]^-$, $[MoCp(CO)_3]^-$ and $[Fe(CO)_4]^{2-}$ are of course applicable to other isoelectronic, 18e carbonylmetallates and our approach allows to connect diverse, seemingly very different molecules, and provides a global picture endowed with a predictive power.

## Acknowledgements

We thank the CNRS and the MESS. Krüger, H.-J. Kraus, *Chem. Ber.* **1986**, *119*, B.Z. are grateful to the Algerian DGRS-DT for financial support. P.B. is grateful to the coworkers and collaborators cited in the references for their dedicated contributions to the development of the topic. We are grateful to the referees for their careful reading of the manuscript.

**Keywords:** metal clusters • metal-metal bonds • metal carbonyl fragments • electron counts • density functional theory

### References

[1] P. Braunstein, L. A. Oro, P. R. Raithby, *Metal Clusters in Chemistry, Vol. 1-3*, Wiley-VCH, Weinheim, **1999**.
[2] R. E. Dessy, P. M. Weissman, *J. Am. Chem. Soc.* **1966**, *88*, 5124-5129.
[3] G. M. Sheldrick, R. N. F. Simpson, *Chem. Comm.* **1967**, 1015-1015.
[4] W. Hieber, *Adv. Organomet. Chem.* **1970**, 1-28.
[5] E. W. Comprehensive Organometallic Chemistry II; Abel, Stone, F. G. A., Wilkinson, G., Eds., *Comprehensive Organometallic Chemistry II, Vol. 10*, Pergamon Press: Oxford, 1995.
[6] Metal-Metal Bonding, in *Struct. Bond., Vol. 136* (Ed.: G. Parkin), Springer-Verlag Berlin Heidelberg, **2010**.
[7] S. Sculfort, P. Braunstein, *Chem. Soc. Rev.* **2011**, *40*, 2741-2760.
[8] J. E. McGrady, Introduction and General Survey of Metal–Metal Bonds, in *Molecular Metal-Metal Bonds: Compounds, Synthesis, Properties* (Ed.: S. T. Liddle), Wiley-VCH, Weinheim, **2015**, pp. 1-22.
[9] P. Braunstein, A. A. Danopoulos, *Chem. Rev.* **2021**, *121*, 7346-7397.
[10] C. E. Coffey, J. Lewis, R. S. Nyholm, *J. Chem. Soc.* **1964**, 1741-1749.
[11] P. Braunstein, J. Dehand, *J. C. S. Chem. Comm.* **1972**, 164-165.
[12] P. Braunstein, J. Dehand, *J. Organomet. Chem.* **1975**, *88*, C24-C26.
[13] P. Braunstein, U. Schubert, M. Burgard, *Inorg. Chem.* **1984**, *23*, 4057-4064.
[14] S. Sculfort, R. Welter, P. Braunstein, *Inorg. Chem.* **2010**, *49*, 2372-2382.
[15] P. Braunstein, J. Dehand, *J. Organomet. Chem.* **1970**, *24*, 497-500.
[16] J.-P. Barbier, P. Braunstein, *J. Chem. Research-S* **1978**, 412-413.
[17] R. J. Pearson, J. Dehand, *J. Organomet. Chem.* **1969**, *16*, 485−490.
[18] P. Braunstein, J. Dehand, *J. Organomet. Chem.* **1970**, *81*, 123-137.
[19] P. Braunstein, J. Dehand, *C. R. Acad. Sc. Paris* **1972**, *274*, 175-177.
[20] P. Braunstein, J. Dehand, *J. Organomet. Chem.* **1974**, *81*, 123–137.
[21] O. Bars, P. Braunstein, J.-M. Jud, *New J. Chem.* **1984**, *8*, 771-776.
[22] P. Braunstein, G. Predieri, F. J. Lahoz, A. Tiripicchio, *J. Organomet. Chem.* **1985**, *288*, C13-C16.
[23] R. Bender, P. Braunstein, Y. Dusausoy, J. Protas, *Angew. Chem. Int. Ed. Engl.* **1978**, *17*, 596-597.
[24] R. Bender, P. Braunstein, Y. Dusausoy, J. Protas, *J. Organomet. Chem.* **1979**, *172*, C51-C54.
[25] R. Bender, P. Braunstein, J. M. Jud, Y. Dusausoy, *Inorg. Chem.* **1983**, *22*, 3394-3407.
[26] R. Bender, P. Braunstein, J. M. Jud, Y. Dusausoy, *Inorg. Chem.* **1984**, *23*, 4489-4502.
[27] D. M. P. Mingos, *Acc. Chem. Res.* **1984**, *17*, 311-319.
[28] D. M. P. Mingos, D. J. Wales, *Introduction to cluster chemistry*, Prentice Hall, Englewood Cliffs, N.J., **1990**.
[29] P. Braunstein, C. de Bellefon, S.-E. Bouaoud, D. Grandjean, J.-F. Halet, J.-Y. Saillard, *J. Am. Chem. Soc.* **1991**, *113*, 5282-5292.
[30] D. M. P. Mingos, *J. Chem. Soc., Chem. Commun.* **1983**, 706-708.
[31] D. M. P. Mingos, D. G. Evans, *J. Organomet. Chem.* **1983**, *251*, C13-C16.
[32] N. J. Taylor, P. C. Chieh, A. J. Carty, *J. Chem. Soc., Chem. Commun.* **1975**, 448-449.
[33] R. Bender, P. Braunstein, A. Tiripicchio, M. T. Camellini, *Angew. Chem.-Int. Ed. Engl.* **1985**, *24*, 861-862.
[34] R. Bender, P. Braunstein, A. Dedieu, P. D. Ellis, B. Huggins, P. D. Harvey, E. Sappa, A. Tiripicchio, *Inorg. Chem.* **1996**, *35*, 1223-1234.
[35] R. Bender, R. Welter, P. Braunstein, *Inorg. Chim. Acta* **2015**, *424*, 20-28.
[36] H. Werner, A. Kühn, *Angew. Chem. Int. Ed. Engl.* **1977**, *16*, 412–413.
[37] H. Werner, A. Kühn, *Z. Naturforsch.* **1978**, *33b*, 1360-1364.
2777-2795.
[39] H. Werner, H.-J. Kraus, P. Thometzek, *Chem. Ber.* **1982**, *115*, 2914-2926.
[40] P. Thometzek, H. Werner, *J. Organomet. Chem.* **1983**, *252*, C29-C34.
[41] C. Archambault, R. Bender, P. Braunstein, S.-E. Bouaoud, D. Rouag, S. Golhen, L. Ouahab, *Chem. Commun.* **2001**, 849-850.
[42] R. Hoffmann, *Angew. Chem. Int. Ed. Engl.* **1982**, *21*, 711-724.
[43] M. Elian, M. M. L. Chen, D. M. P. Mingos, R. Hoffmann, *Inorg. Chem.* **1976**, *15*, 1148-1155.
[44] R. Bender, P. Braunstein, B. Metz, P. Lemoine, *Organometallics* **1984**, *3*, 381-384.
[45] R. Bender, P. Braunstein, S. E. Bouaoud, D. Rouag, P. D. Harvey, S. Golhen, L. Ouahab, *Inorg. Chem.* **2002**, *41*, 1739-1746.
[46] P. Braunstein, J. Fischer, D. Matt, M. Pfeffer, *J. Am. Chem. Soc.* **1984**, *106*, 410-421.
[47] G. te Velde, F. M. Bickelhaupt, E. J. Baerends, C. Fonseca Guerra, S. J. A. van Gisbergen, J. G. Snijders, T. Ziegler, *J. Comput. Chem.* **2001**, *22*, 931-967.
[48] ADF2020, Theoretical Chemistry, VrijeUniversiteit: Amsterdam, The Netherlands; http://www.scm.com.
[49] K. Morokuma, *J. Chem. Phys.* **1971**, *55*, 1236–1244.
[50] K. Kitaura, K. Morokuma, *Int. J. Quantum Chem* **1976**, *10*, 325-340.
[51] T. Ziegler, A. Rauk, *Inorg. Chem.* **1979**, *18*, 1558-1565.
[52] T. Ziegler, A. Rauk, *Inorg. Chem.* **1979**, *18*, 1755-1759.
[53] F. M. Bickelhaupt, E. J. Baerends, *Rev. Comput. Chem.* **2000**, *15*, 1-86.
[54] T. A. Albright, J. K. Burdett, M.-H. Whangbo, *Orbital Interactions in Chemistry, 2nd edition*, John Wiley & Sons, Inc: New York, **2013**.
[55] P. Braunstein, A. Müller, H. Bögge, *Inorg. Chem.* **1986**, *25*, 2104-2106.
[56] P. Braunstein, J. Dehand, *Bull. Soc. Chim. Fr.* **1975**, 1997-2003.
[57] P. Braunstein, E. Keller, H. Vahrenkamp, *J. Organomet. Chem.* **1979**, *165*, 233-242.
[58] P. Braunstein, E. Cura, G. E. Herberich, *J. Chem. Soc. Dalton* **2001**, 1754-1760.
[59] P. Croizat, N. Auvray, P. Braunstein, R. Welter, *Inorg. Chem.* **2006**, *45*, 5852-5866.

[60] P. Klüfers, *Angew. Chem. Int. Ed. Engl.* **1984**, *23*, 307-308.
[61] P. Klüfers, *Z. Kristallogr. - Cryst. Mater.* **1984**, *166*, 143–151.
[62] S. Sculfort, P. Croizat, A. Messaoudi, M. Benard, M.-M. Rohmer, R. Welter, P. Braunstein, *Angew. Chem. Int. Ed.* **2009**, *48*, 9663-9667.
[63] P. Croizat, S. Sculfort, R. Welter, P. Braunstein, *Organometallics* **2016**, *35*, 3949-3958.
[64] G. Doyle, K. A. Eriksen, D. Vanengen, *J. Am. Chem. Soc.* **1986**, *108*, 445–451.
[65] V. G. Albano, F. Azzaroni, M. C. Iapalucci, G. Longoni, M. Monari, S. Mulley, D. M. Proserpio, A. Sironi, *Inorg. Chem.* **1994**, *33*, 5320-5328.
[66] B. Berti, M. Bortoluzzi, C. Cesari, C. Femoni, M. C. Iapalucci, R. Mazzoni, F. Vacca, S. Zacchini, *Inorg. Chem.* **2019**, *58*, 2911-2915.
[67] V. G. Albano, L. Grossi, G. Longoni, M. Monari, S. Mulley, A. Sironi, *J. Am. Chem. Soc.* **1992**, *114*, 5708-5713.
[68] V. G. Albano, F. Calderoni, M. C. Iapalucci, G. Longoni, M. Monari, P. Zanello, *J. Cluster Sci.* **1995**, *6*, 107-123.
[69] S. Kahlal, C. W. Liu, J. Y. Saillard, *Inorg. Chem.* **2017**, *56*, 1209-1215.
[70] D. E. Crotty, E. R. Corey, T. J. Anderson, M. D. Glick, J. P. Oliver, *Inorg. Chem.* **1977**, *16*, 920-924.
[71] R. Janta, W. Albert, H. Rößner, W. Malisch, H.-J. Langenbach, E. Röttinger, H. Vahrenkamp, *Chem. Ber.* **1980**, *113*, 2729-2738.

10.1002/chem.202203557

WILEY-VCH

RESEARCH ARTICLE

## Entry for the Table of Contents

Easy Rationalization of the Structure of **Metal Clusters** by Considering 18e Carbonylmetallates [m]$^-$ as Pseudohalides, Acting as Terminal, Doubly or Triply-Bridging **2-, 4- or 6e Donor Metalloligands**, **respectively.**

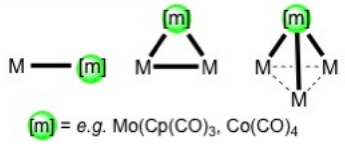


The structure of various heterometallic carbonyl clusters containing metals that do not follow typical electron-counting rules can be readily explained by considering their constitutive 18e metal carbonyl fragment [m]$^-$ as a pseudo-halide, also similar to phosphido or allyl ligands.

Institute and/or researcher Twitter usernames: ((optional))